

ABSTRACTS OF PAPERS

presented at the Annual Symposium of the SRBR - KBVR, on November 16, 2013

SAMENVATTINGEN VAN DE UITEENZETTINGEN

voorgesteld aan het Jaarlijks Symposium van de KBVR, op 16 november 2013

RESUMES DES COMMUNICATIONS

présentées lors du Symposium Annuel de la SRBR, le 16 novembre 2013

A short history of the Royal Belgian Radiological Society : from skeletal X-rays to whole body imaging J. Pringot¹

Founded in 1895 as the Belgian Radiological Society by a handful of enthusiastic surgeons and physicians, the current Royal Belgian Radiological Society (RBRS) has grown into a vibrant mainly scientific society with more than thirteen hundred members. Due to the remarkable contribution of its members, mastering without delay the technological and technical innovations and their clinical expertise, the RBRS has consolidated its influence not only nationally but also internationally mainly through its affiliation with the European Society of Radiology and the organization of the International (global) Congress of Radiology on Brussels in 1981. Remaining a national organization, it has maintained a critical manpower fostering mutual emulation for excellence in research and clinical work. In consideration of the trend towards sub-specialization initiated by neuroradiology, different subspecialized sections have been created and more recently a rapprochement with the more professionally oriented organization the National Union of Radiologists is on its way. Without going into much detail the historical development of the RBRS will be revisited and major events highlighted during four successive periods: before WWI, between WWI and WWII, from the end of WWII to the sixties, and from the seventies to today. Finally, future possible challenges will be envisaged.

1. Editor-in-Chief JBR-BTR, Professor of Radiology, Consultant radiologist Clinique St Elisabeth, Avenue De Fré 206, 1180 Brussels.

Anterior skull base and olfactory apparatus Th. Duprez¹

Imaging modalities for olfactory work-up

MRI is the best suited imaging modality for cranial nerves imaging.

The capability of MRI to give accurate and reproducible measurements of the bulb triggered the inclusion of the technique into the multi-modal work-up of olfactory disorders. Our standard examination protocol includes 1.5-mm-thick T2-weighted images in Fast Spin-Echo (FSE) mode in the coronal plane which is the best suited technique for anatomical olfactory overview, parenchymal lesion detection, and olfactory bulb (OB) volumetry. Whole brain coverage remains mandatory for detecting parenchymal contusions. We defined the normal range of OB volume from about 40 to 60 mm³ in a 'local' normative cohort. Such variation may be explained by differences in measurement technique but also by intrinsic variations due to the MR system characteristics, post-processing consoles, and computer programs used for measurements. We advocate the use the same MR system for all olfactory tract (OT) examinations, to use the same contouring technique on the same post-processing console – to be done by sufficiently experienced operators –, and ultimately to recruit a normative cohort of sex- and age-related normal controls to build a 'local' reference. We prefer 3T imaging for olfactory imaging but did not find significant penalty to 1.5T images when compared to 3T ones. Residual indication for high-resolution CT is trauma because of exquisite depiction of bone, but with the inherent limitation of limited soft tissue contrast. The absence of relevant soft tissue information – except for mucosal thickening – precludes the routine use of Cone Beam CT (CB-CT) for olfactory disorders, except when bone work-up is restrictively desired. X-Ray plain films have obviously become obsolete and catheter angiography, MRA, CTA and PET-CT have no primary indications in the purpose.

Overview of olfactory tract disorders

Congenital anosmia

Patients who say they have never had any sense of smell and in whom

olfactory dysfunction is assessed by functional tests are reputed as 'congenitally anosmics' after ruling out any acquired cause for olfactory dysfunction. MR examination may demonstrate severely hypoplastic or absent OB together with flattening or even absence of olfactory sulcus. Congenital anosmia may be isolated or associated to hypogonadotropic hypogonadism in the so-called Kallmann's syndrome.

Idiopathic olfactory loss

Patients who are consulting for olfactory loss and who declare to have had 'normal' sense of smell before the present episode are reputed to have 'idiopathic' olfactory loss (IOL) when all common causes for the condition have been ruled out. Those patients have significantly decreased OB volumes when compared with a mirror cohort of sex- and age-matched control.

Non neoplastic acquired olfactory loss

1. Trauma

Trauma is a leading cause of olfactory dysfunction. Parenchymal posttraumatic lesions can be observed throughout the OT at MRI, and bone disruption at CT scanner. In some cases, the imaging work-up fails to reveal any damage to the olfactory pathways, except atrophy of the OB which is putatively secondary to de-afferentiation because of the shear-injury of the olfactoria fila on their way through the cribriform plates of ethmoid. Strong relationship between OB volume and post-traumatic olfactory dysfunction has already been evidenced by many studies.

2. Infection

Patients complaining from post-infectious olfactory loss are usually middle-aged women who suffer from persisting smell disturbances in the disease course of an acute – probably viral – upper airways infection. The sense of smell is usually decreased both quantitatively (hyposmia) and qualitatively with

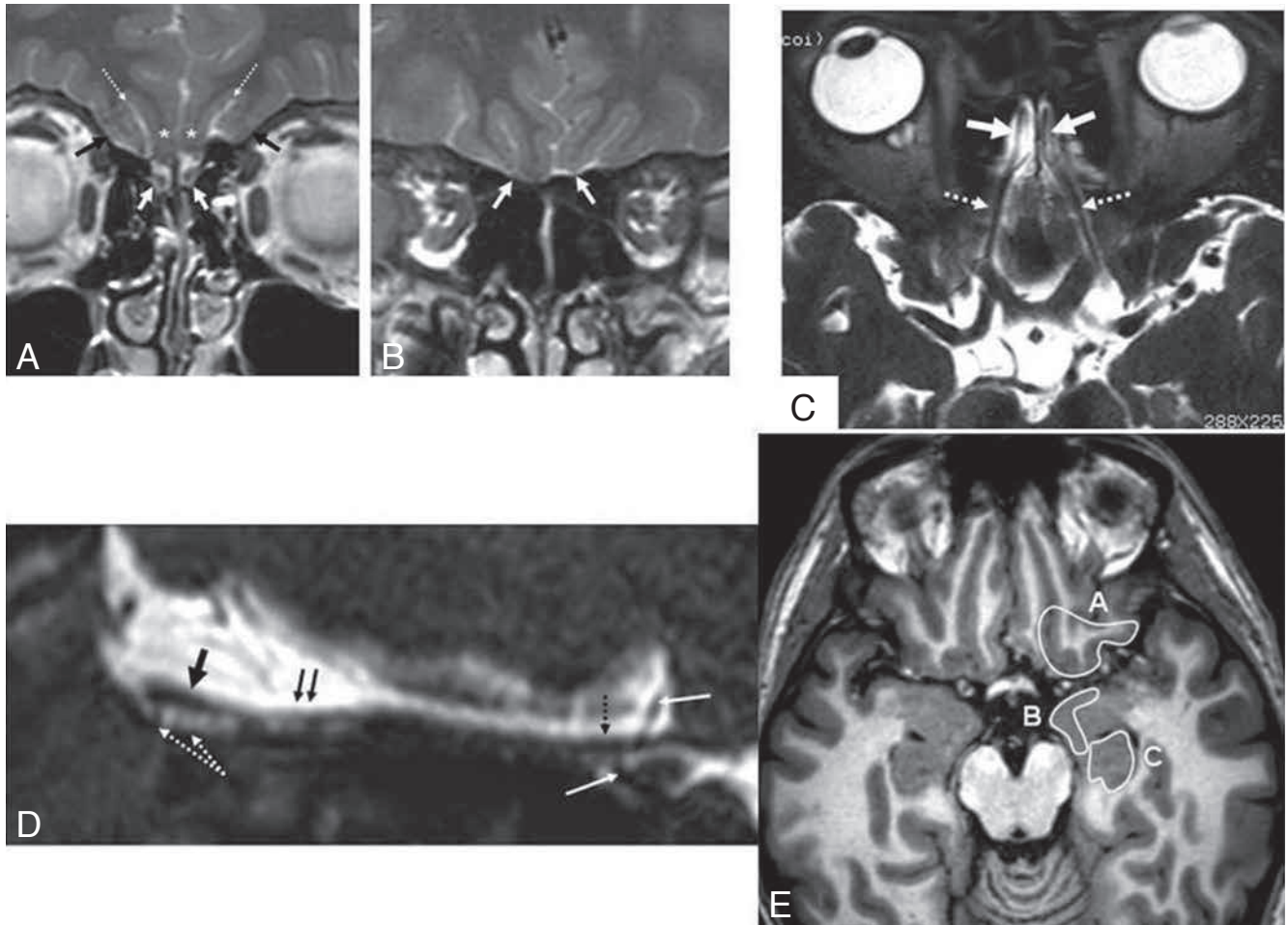


Fig. 1. — MR anatomy of the olfactory tract (from reference #1, with permission). A. Coronal 2D 2-mm-thick T2-weighted slice through olfactory bulbs (OB) in Fast Spin Echo technique (FSE). Hypointense OBs surrounded by bright cerebrospinal fluid (CSF) are well seen within olfactory grooves (OG) of ethmoid bone on both sides of the midline (white arrows). Gyri recti (white stars) are separated from the adjacent medial orbital gyri (black arrows) by the olfactory sulci (OS) (thin dotted arrows). B. Coronal 2D 2-mm-thick FSE T2-weighted slice in a more posterior location than previous view showing thinner olfactory tracts (OT) (arrows). C. Transverse reformatted view of a 3D FSE T2-weighted sequence using driven equilibrium (DRIVE[®]) acquisition showing OBs (arrows) and the OTs (dotted arrows) running through olfactory grooves (OG) at inferior border of gyri recti and medial orbital gyri. D. Sagittal reformat of the same 3D FSE T2-weighted DRIVE sequence than in previous image showing the olfactory tract as a whole from OB to cribriform substance. Observe well delineation of OB (black arrow), proximal (paired arrows) and distal (dotted arrow) OT, but poor individualization of its intermediate segment because of its close contiguity to the bone. Olfactory filia linking the extra-cranial olfactory neuro-epithelium to the OBs through the openings of ethmoid cribriform plates are well seen (white dotted arrows). The presence of thin crossing vessels (thin white arrows) may be confusing as shown in Fig. 5. E. Main central projection areas of the sense of smell drawn on a transverse T1-weighted section: orbitofrontal olfactory area (A) is the main central neo-cortical projection having thalamic inter-connections through medial dorsal nucleus. Piriform (B) and entorhinal (C) cortices are prominent paleo-cortical projection areas without intermediate thalamic connections.

misinterpretation of odours (parosmia).

Chronic rhinosinusitis

Patients with chronic rhinosinusitis (CRS) frequently complain from olfactory impairment. Dysfunction of the olfactory neuroepithelium due to interaction with mucosal inflammatory mediators and physical impossibility for odorant molecules to reach the olfactory cilia due to obstruction, mucosal edema, and polyp formation are putatively synergistic mechanisms for the disorder.

Patients with slight to moderate inflammation of paranasal sinuses had significantly larger OB volumes than patients with higher-grade CRS.

Intrinsic olfactory tract neoplasms

Schwannomas of the OT can be observed because of the presence of ensheating glial cells within olfactory glomeruli. Esthesioneuroblastoma is the paradigmatic neuroblastoma of the 1st cranial nerve which may arise from either the nasal olfactory neuroepithelium or from the intra-cranial OT.

Extrinsic benign neoplasms impinging on the OT

Meningiomas are frequently observed benign tumors causing smell dysfunction. The tumor size and the degree of lesion impingement on OT are poorly related to the severity of smell complaints.

Malignancies invading the olfactory tract.

Ethmoid carcinoma and meningeal carcinomatosis are most frequently involved malignancies in secondary olfactory dysfunction by local invasion.

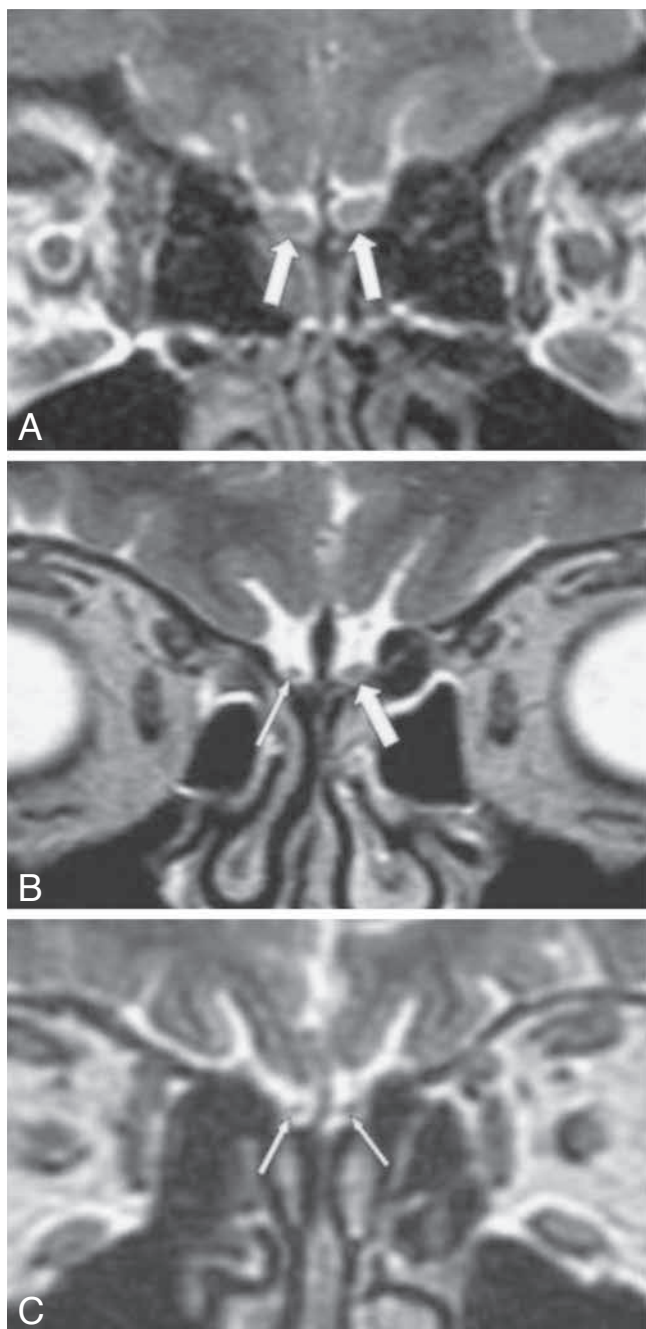


Fig. 2. — Post-viral damage to the OT (from reference #1, with permission). 2 mm-thick FSE T2-weighted coronal views in all three cases. A. Normal control with eutrophic OB on both sides (thick arrows). B. Patient with post-viral hyposmia exhibiting asymmetric atrophy of the OBs, the right-sided one (thin arrow) being more damaged than the left-sided one (thicker arrow). C. Patient with severe anosmia and cacosmia showing symmetrical severe atrophy of OBs (thin arrows).

Neurodegenerative disorders

Many studies have highlighted early olfactory disturbance in patients with idiopathic Parkinson's disease (IPD) or with Alzheimer's disease (AD). Decreased OB volumes may precede for several years the

onset of other symptoms than olfactory dysfunction.

Conclusions

Quantitative measures of olfactory bulb volume and morphological depiction of structural abnormalities

synergistically contributes to accurate radiological diagnosis and prognosis of smell disturbances.

References

1. Duprez T.P., Rombaux P.: Imaging the olfactory tract (cranial nerve #1). *Eur J Radiol*, 2010, 74: 288-298.
2. Buschhüter D., Smitka M., Puschmann S., Gerber J.C., Witt M., Abolmaali N.D., Hummel T.: Correlation between olfactory bulb volume and olfactory function. *NeuroImage*, 2008, 42: 498-502.

1. Department of Radiology and Medical Imaging, Université Catholique de Louvain, Cliniques Universitaires Saint-Luc, Brussels.

Interventional radiology in the head and the neck

H. Tanghe¹

The indications for vascular interventions in the Head and the Neck are:

1. Intractable epistaxis.
2. Penetrating neck trauma.
3. Craniofacial vascular lesions.
4. Preoperative tumor embolization.
5. Rupture of vessels, damaged by cancer or infection.
6. (Carotid stenting).

Epistaxis is a common, usually benign and self-limiting disease. Anterior epistaxis is the most common type. The bleeding comes from the anterior septum, locus Kesselbachi and does not require special treatment. Posterior epistaxis comes from the fossa nasalis posterior or posterior septum. It is rare and requires active treatment. Intractable epistaxis is defined as a nosebleed that does not respond to posterior nasal packing. The treatment of choice is embolization, with a success rate of 90%.

Penetrating neck trauma can cause multiple vessel lesions in the neck and of course other parenchymal, vertebral and spinal cord lesions. Don't be satisfied when you have found one vascular lesion The best diagnostic imaging method is a CT-angiography. Indication for endovascular treatment are: serious bleeding from a branch vessel, bleeding from a hole in the side wall of a major vessel, bleeding from a transection of a major vessel, traumatic A-V fistula. The technique used depends on the situation.

Craniofacial vascular lesions are classified as vascular proliferations

or vascular malformations. Several interventional techniques are possible: a direct puncture approach, an endovascular approach, with a variety of possible agents. Combined treatment with plastic surgery is common.

Preoperative tumour embolization is indicated in paraganglioma, juvenile angiofibroma. The goal is the diminution of the preoperative blood loss, the shortening the operation time, the easier identification of surgical important structures and a to achieve a higher rate of radical tumour removal. The principle of a preoperative tumor embolization is the selective obliteration of the intratumor vasculature, while preserving the normal supply to the surrounding tissues. Thus a distal occlusion of a feeding vessel is not appropriate. You must be aware of the multiple dangerous connection that exists between the external carotid territory on the one side and the internal carotid and vertebral territory on the other side.

Sudden non traumatic rupture of a major neck artery can occur in advanced head and neck cancer and in severe infections, like necrotizing otitis externa ("malignant otitis externa) with expansion to the carotid loge. It is always a debate in a specific patient, yes or not, to treat this emergency situation, giving the prognosis of the underlying disease, the problems of catheterisations and the frequent poor clinical condition of these patients.

Carotid or vertebral stenting for the treatment of stenotic atherosclerotic disease in the major neck arteries is almost gone today, as also the skills of the people who did these procedures several years ago. The indications nowadays are limited.

1. Section of Neuroradiology / Head & Neck Radiology, Department of Radiology, Erasmus Medical Centre, Rotterdam, The Netherlands, Postbus 2040, 3000 CA Rotterdam, The Netherlands.
E-mail: h.l.j.tanghe@erasmusmc.nl

Tracheal imaging

W. De Wever¹

Chest X-ray is traditionally the first step in the evaluation of tracheal disease. However, tracheal disease is usually overlooked initially on radiography. The spectrum of tracheal disorders is diverse. Abnormalities of the trachea can be classified as congenital, infectious, inflammatory,

infiltrative, traumatic or neoplastic. Diseases of the trachea can be focal or diffuse and can cause luminal widening or luminal narrowing. The diagnosis and differential diagnosis of tracheal disease is based on the appearance of the tracheal wall on inspiratory CT scans, on changes in the tracheal wall during expiration, and on the location and extent of the tracheal abnormalities. Axial, thin, inspiratory and expiratory CT images are the standard of reference for the evaluation of tracheal disease. Two-dimensional multiplanar reformations are useful for the evaluation of the extent of these abnormalities.

Anatomy of the trachea

The trachea is a cartilaginous and fibromuscular tube-structure. In the chest, in general, the trachea is midline in position, often displaced slightly to the right at the level of the aortic arch. It extends from the level of the cricoid cartilage (level of C6) to the carina, (level of T4-T5). At the carina the trachea bifurcates into left and right main stem bronchus (1). The trachea is divided into an extra-thoracic and an intra-thoracic part at the point where it passes posteriorly to the manubrium. In adults, the length of the trachea on CT, measured during inspiration, is approximately 11-13 cm. The extra-thoracic part measures 2 to 4 cm (2). The shape of the trachea during inspiration is semi-oval with a coronal diameter of 13 to 25 mm in men and 10 to 21 mm in women, and a sagittal diameter of 13 to 27 mm in men and 10 to 23 mm in women (2). Measurement error of the tracheal diameter can occur if the measurement is not perpendicular to the plane of scanning. The tracheal index can be calculated as a ratio of the coronal diameter (mm) by the sagittal diameter (mm). The normal value is approximately one (3). The anterior and lateral wall of the trachea is composed by 16 to 22 horseshoe bands of cartilage. From inside out, the tracheal wall is composed of several layers: mucosa, submucosa, cartilage or muscle, and adventitia. The posterior tracheal wall lacks cartilage and is made of a thin membrane supported by the trachealis muscle (4). On CT, the tracheal wall appears as a 1 to 3 mm soft tissue stripe outlined by air in the lumen and mediastinal fat on the outer side. The posterior wall appears thinner and gives a variable contour to the shape of the trachea due to the lack of cartilage. The posterior wall can appear flat, convex or

slightly concave depending on the level of inspiration (2). The posterior wall of the trachea either flattens or bows slightly forward during expiration. In normal subjects there is up to a 35% reduction in AP tracheal lumen in forced expiration, whereas the transverse diameter decreases only by 13% (5). The angle of the tracheal bifurcation, also called the carinal angle, can vary. The carinal angle is wider in individuals with an enlarged left atrium, in females, in obese patients, and in people with the carina located closer to the spine (1).

Imaging modalities

The plain chest radiograph is traditionally the first step in the evaluation of tracheal disease. However radiography is relatively insensitive to airway changes and large airway disease is overlooked initially (6).

The diagnosis of tracheal disease is often based on the appearance of the tracheal wall on inspiratory scans, changes in the tracheal wall with expiration, and the location and extent of tracheal abnormalities (4). Computed tomography (CT) can improve the detection and characterization of tracheal disease, and multidetector CT (MDCT) is the imaging modality of choice for the diagnosis of tracheal disease (7). The newer multidetector scanners of 64-128 rows of detector and collimators as thin as 0.625 create a near isometric resolution voxel of 0.4 mm. Slices are reconstructed, with 50% overlap, in the transaxial plane. A rotation time of approximately 500 ms allows a significant decrease in cardiac pulsation artifacts and allows a good analysis of the trachea. State-of-the-art, 320-detector CT scanners can cover 16 cm of tissue in 350 ms, and hence can image the entire trachea with just a single gantry rotation and allow for dynamic cine imaging of the trachea during respiration. MDCT scanners generate an isotropic voxel data set, which allows for the creation of high-resolution, 2-dimensional multiplanar, and 3D image reconstructions of the trachea in simply a few minute. The unique inherent natural contrast of the airways and lung parenchyma permits imaging with a relatively lower radiation dose without significant loss of information (100-120 kV, 60-160 mAs). Imaging is obtained in suspended inspiration (2) (8, 9).

Axial CT images provide precise anatomical information about the airway lumen and wall, as well as

about adjacent mediastinal and lung structures. Multiplanar 2-dimensional reformations and 3-dimensional reconstruction images can provide a more anatomically meaningful display of the airways and adjacent structures. These CT images have been shown to enhance the detection, localization, and determination of the extent of lesions; the evaluation of their relationship with adjacent structures; characterization of the airway disease; and clarification of complex congenital airway abnormalities (10).

Axial CT imaging

Axial CT images serve today as the reference standard for the imaging of the trachea because this imaging technique can evaluate the wall of the trachea in the best way. This imaging technique provide detailed information of the size and shape of the airway, wall thickness, presence of calcification, presence of intraluminal lesions, and delineate the relationship of the airways to adjacent mediastinal structures. However, on axial CT images, subtle stenoses of the trachea can be overlooked, the craniocaudal extent of a disease may be inaccurate estimated, complex airway anatomy may be poorly defined, and evaluation of airways oblique to the axial plane may be limited. Expiratory or dynamic expiratory scans may be obtained after or during forced exhalation to show tracheomalacia (2, 4, 11).

Two-dimensional multiplanar reformation

2D multiplanar reformation images of the airways serve as a diagnostic complement to the axial source images and can be simply and interactively generated in real time at the CT console or workstation. Two-dimensional multiplanar reformation images can be displayed in a coronal, sagittal or oblique plane or curved reformations along the long axis of the airways. Two-dimensional multiplanar reformation images improve the detection of airway stenoses, precisely define airway disease extent in multiple planes, clarify complex congenital airway abnormalities, and may help identify sites of airway disruption (11).

Multiple adjacent thin slices can be stacked together to generate a thick slab or multiplanar volume reformation image. Slice thickness can be altered to any dimension. In general, slice thicknesses of 3 to 7 mm give adequate image information. Minimum intensity projection (mIP) projects the pixels with the lowest attenuation values in a 2-D format. The trachea-bronchial tree and any lucent abnormalities, such as diverticula or fistulous communications, can be displayed well on mIP reconstructions (11, 12).

3D reconstruction

3D reconstructions include external and internal renderings of the airways. External 3D rendering of the

airways is equivalent to CT bronchography. With his technique, the inner surface of the trachea and airways can be depicted and their relationship with adjacent structures can be demonstrated. 3D segmentation provides a rapid anatomic overview of the airways. Recognition of mild and focal airway stenoses, and more relevant information on the shape, length, and severity of these stenoses can be provided in an easy way (11).

Internal 3D rendering of the airways is equivalent to virtual bronchoscopy (VB). This VB enables the viewer to navigate through the lumen of the airway to the sixth-order and seventh-order subdivisions. VB is a useful noninvasive method of assessment of airway stenoses, which cannot be evaluated on conventional bronchoscopy when passing the stenosis is impossible. VB may obviate the need for invasive conventional bronchoscopy in certain circumstances and in special subgroups of patients such as young children, very sick patients or elderly patients who may not be able to tolerate bronchoscopy. VB does not permit tissue sampling, which can be done with endoscopic bronchoscopy (11, 13).

Spectrum of tracheal diseases

The spectrum of tracheal disorders is diverse. Abnormalities of the trachea can be classified as congeni-

Table 1. – Spectrum of tracheal diseases.

Tracheal disease	Congenital	Infectious / inflammatory / infiltrative	Traumatic	Neoplastic
Diffuse disease				
Luminal dilatation	<ul style="list-style-type: none"> • Mounier-Kuhn • Ehlers-Danlos syndrome 	<ul style="list-style-type: none"> • Saber-Sheath trachea 		
Luminal narrowing	<ul style="list-style-type: none"> • Tracheal web 	<ul style="list-style-type: none"> • Tracheo-bronchomalacia • Relapsing polychondritis • Wegener granulomatosis • Acute infectious tracheo-bronchitis • Chronic trachea-bronchitis associated with autoimmune diseases • Amyloidosis • Sarcoidosis • Tracheopathia-osteocondroplastica 		
Focal disease				
Luminal narrowing	<ul style="list-style-type: none"> • Tracheal ring • Vascular rings • Pulmonary sling • Mediastinal vascular anomalies 		<ul style="list-style-type: none"> • Idiopathic tracheal stenosis • Intubation related stenosis • Stricture post tracheostomy 	<ul style="list-style-type: none"> • Benign neoplasms • Primary malignant neoplasms • Secondary malignant neoplasms

Table II. — Tracheal diseases: pathology and CT findings.

Tracheal disease	Pathology	Tracheal localization	CT-findings
Saber-Sheath trachea	Weakness of cartilage	Intrathoracic trachea	<ul style="list-style-type: none"> • Decrease of coronal diameter, increase of sagittal diameter • Inward bowing of the tracheal wall • More pronounced on expiratory scans
Acute post-intubation stenosis	<ul style="list-style-type: none"> • Mucosal edema • Granulation tissue 	Intrathoracic trachea	<ul style="list-style-type: none"> • Eccentric or concentric soft tissue thickening on the internal side of the trachea • Normal aspect of the cartilage • Outer tracheal wall has a normal appearance
Chronic stenosis	<ul style="list-style-type: none"> • Weakness of cartilage • Thickening of mucosa and submucosa 	Intrathoracic trachea	<ul style="list-style-type: none"> • Focal tracheal narrowing during or after forced expiration
Wegener's granulomatosis	Mucosal and submucosal inflammation and ulceration	<ul style="list-style-type: none"> • Extrathoracic trachea (subglottis) • Intrathoracic trachea (variable degree) 	<ul style="list-style-type: none"> • Circumferential wall thickening • Narrowing of the tracheal lumen
Amyloidosis	Amyloid deposition in the submucosa	<ul style="list-style-type: none"> • Extrathoracic trachea • Intrathoracic trachea 	<ul style="list-style-type: none"> • Concentric, smooth or nodular thickening of the submucosal wall • Concentric calcification or ossification may occur • No tracheomalacia
Tracheobronchopathia osteochondroplastica	Osseous and/or cartilaginous nodules in the submucosa	<ul style="list-style-type: none"> • Extrathoracic trachea • Intrathoracic trachea 	<ul style="list-style-type: none"> • Nodular thickening of the tracheal wall with calcified nodules on the inner aspect of the lumen • Posterior membrane is normal • Malacia is not present
Tracheobronchomegaly	Atrophy of cartilaginous, muscular and elastic components of the tracheal wall	<ul style="list-style-type: none"> • Extrathoracic trachea • Intrathoracic trachea 	<ul style="list-style-type: none"> • Thinning of the tracheal wall • Tracheal diameter of more than 3 cm at 2 cm above the aortic arch • Tracheal diverticulosis can be seen. • Trachea tends to collapse with forced expiration
Relapsing polychondritis	Inflammation of the cartilage	<ul style="list-style-type: none"> • Extrathoracic trachea • Intrathoracic trachea 	<ul style="list-style-type: none"> • Wall thickening limited to the anterior and lateral tracheal wall • Posterior membrane is spared • Collaps of the cartilage with narrowing of the lumen • Inner and outer border of the thickened tracheal wall are smooth
Recurrent respiratory papillomatosis	Exophytic lesions in the airway	<ul style="list-style-type: none"> • Extrathoracic trachea • Intrathoracic trachea 	<ul style="list-style-type: none"> • Well circumscribed tracheal wall lesions with progressive mass-like protrusions • Airway obstruction may occur • No extension beyond the trachea or bronchial wall
Sarcoidosis	Granulomas in mucosa or submucosa	<ul style="list-style-type: none"> • Extrathoracic trachea • Intrathoracic trachea 	<ul style="list-style-type: none"> • Regular or nodular wall thickening with smooth or irregular luminal narrowing

tal, infectious, inflammatory, infiltrative, traumatic or neoplastic (7). Diseases of the trachea are focal or diffuse, depending on the extent of the disease and cause airway luminal widening or luminal narrowing. Focal diseases causing luminal narrowing include malignant or benign tumor and tracheal strictures caused by trauma or medical intervention. Diffuse luminal narrowing of the airway is caused by various infiltrative and infectious diseases (2). Diseases of the trachea are summarized in Table I. Differential diagnosis is based on the appearance of the tracheal wall on inspiratory and expi-

ratory scans. Recognizing specific tracheal wall abnormalities is of primary importance because specific diseases tend to affect different components. Correlation between pathological findings and CT findings of different tracheal diseases is summarized in Table II.

Saber-sheath Trachea

Saber-Sheath trachea is a common finding and almost always associated with chronic obstructive pulmonary disease. Due to a weakness of the cartilage, this disease is marked by a decrease in the coronal diameter and an increase in the sagittal

diameter with an inward bowing of the tracheal wall. This finding is more expressed on expiratory CT scans. This abnormality is only present at the level of the intrathoracic trachea (2, 4, 7).

Tracheal stenosis

Acute post-intubation stenosis results from mucosal edema or granulation tissue. On CT, an eccentric or concentric soft tissue thickening on the internal side of the trachea with a normal aspect of the cartilage is seen. The outer tracheal wall has a normal appearance. Expiratory CT

images show little change in tracheal diameter. Chronic stenosis post-intubation or tracheostomy shows tracheal narrowing due to deformity of the tracheal cartilage or posterior membrane with or without thickening of the mucosa and submucosa. Tracheomalacia results from weakness of the tracheal cartilage with a narrowing of the intrathoracic trachea on CT during or after forced expiration (2, 4, 14).

Wegener's granulomatosis

Mucosal and submucosal inflammation and ulceration involves the trachea. Subglottic involvement is most typical with a variable involvement of the distal trachea. Destruction of the tracheal cartilage may occur. Axial CT images show a circumferential wall thickening and narrowing of the tracheal lumen (2, 4, 7).

Amyloidosis

Tracheobronchial amyloidosis is a rare condition. Amyloid is deposit in the submucosa. The entire trachea is involved. On CT, diffuse amyloidosis leads to concentric, smooth or nodular thickening of the submucosal tracheal wall. The tracheal cartilage is normal, but concentric calcification or ossification may occur. There is no tracheomalacia (4, 7).

Sarcoidosis

Sarcoidosis is a systemic disease of unknown cause. Large airway involvement is unusual. Sarcoidosis will affect the larynx and upper trachea in 1% to 3% of patients. The distal part of the trachea is affected infrequently. Narrowing of the airway may be secondary to extrinsic compression from enlarged lymph nodes or may be the result of granuloma formation within the airway mucosa and submucosa. The most common CT finding is regular or nodular wall thickening. This may result in smooth or irregular luminal narrowing (7, 15).

Tracheobronchopathia osteochondroplastica

Tracheobronchopathia osteochondroplastica is characterized by development of osseous or cartilaginous nodules or both in the submucosa. These nodules are associated with tracheal cartilage, sparing the posterior membrane. CT findings include thickening of the tracheal wall with small calcified nodules along the inner aspect of the lumen

with protruding into the tracheal lumen. Malacia is not present (4).

Mounier-Kuhn syndrome (Tracheobronchomegaly)

Tracheobronchomegaly is a rare condition characterized by marked dilatation of the trachea and mainstem bronchi. Tracheobronchomegaly is characterized by atrophy of cartilaginous, muscular and elastic components of the tracheal wall. Axial CT images show a thinning of the tracheal wall and a tracheal diameter of more than 3 cm at 2 cm above the aortic arch. Tracheal diverticulosis can be seen. The trachea tends to collapse with forced expiration (2, 4, 7).

Relapsing Polychondritis

Relapsing polychondritis is characterized by recurrent episodes of cartilage inflammation. Diffuse tracheal inflammation is limited to the cartilage and perichondrium and does not affect the mucosa and submucosa. CT usually shows wall thickening limited to the anterior and lateral tracheal wall. The posterior membrane is spared. There is collapse of the cartilage with narrowing of the lumen. Calcification of the cartilage can be present. The inner and outer borders of the thickened tracheal wall are smooth. The luminal narrowing may be fixed or tracheomalacia may be present (4, 7).

Recurrent respiratory papillomatosis (RRP)

RRP is the result of infection of the upper respiratory tract by human papilloma virus. RRP is characterized by benign exophytic lesions in the airway, most commonly involving the larynx and central trachea-bronchial tree. The lesions give rise to tracheal wall irregularities with progressive mass-like protrusions. Airway obstruction may occur. These lesions tend to be well circumscribed and do not give rise to extension beyond the trachea or bronchial wall (2).

Conclusion

Recent advantages in CT technology and post-processing techniques allow for a noninvasive and accurate evaluation of the trachea. In particular, axial CT images are essential for the evaluation of the tracheal wall. Two-dimensional multiplanar reformations are useful for the evaluation of the extent of tracheal abnormalities.

References

1. Minnich D.J., Mathisen D.J.: Anatomy of the trachea, carina, and bronchi. *Thorac Surg Clin*, 2007, 17: 571-585.
2. Laroia A.T., et al.: Modern imaging of the tracheo-bronchial tree. *World J Radiol*, 2010, 2: 237-248.
3. Grenier P.A., et al.: Multidetector-row CT of the airways. *Semin Roentgenol*, 2003, 38: 146-157.
4. Webb E.M., Elicker B.M., Webb W.R.: Using CT to diagnose nonneoplastic tracheal abnormalities: appearance of the tracheal wall. *AJR Am J Roentgenol*, 2000, 174: 1315-1321.
5. Ederle J.R., et al.: Evaluation of changes in central airway dimensions, lung area and mean lung density at paired inspiratory/expiratory high-resolution computed tomography. *Eur Radiol*, 2003, 13: 2454-2461.
6. Kwong J.S., Muller N.L., Miller R.R.: Diseases of the trachea and mainstem bronchi: correlation of CT with pathologic findings. *Radiographics*, 1992, 12: 645-657.
7. Kang E.Y.: Large airway diseases. *J Thorac Imaging*, 2011, 26: 249-262.
8. Boiselle P.M.: Imaging of the large airways. *Clin Chest Med*, 2008, 29, 181-193, vii.
9. Boiselle P.M., Lee K.S., Ernst A.: Multidetector CT of the central airways. *J Thorac Imaging*, 2005, 20: 186-195.
10. Chen Q., et al.: Evaluation of tracheobronchial diseases: comparison of different imaging techniques. *Korean J Radiol*, 2000, 1: 135-141.
11. Lee K.S., Boiselle P.M.: Update on multidetector computed tomography imaging of the airways. *J Thorac Imaging*, 2010, 25: 112-124.
12. Beigelman-Aubry C., Brillet P.Y., Grenier P.A.: MDCT of the airways: technique and normal results. *Radiol Clin North Am*, 2009, 47: 185-201.
13. De Wever W., et al.: Multidetector CT-generated virtual bronchoscopy: an illustrated review of the potential clinical indications. *Eur Respir J*, 2004, 23: 776-782.
14. Lee K.S., et al.: Multislice CT evaluation of airway stents. *J Thorac Imaging*, 2005, 20: 81-88.
15. Bartz R.R., Stern E.J.: Airways obstruction in patients with sarcoidosis: expiratory CT scan findings. *J Thorac Imaging*, 2000, 15: 285-289.

1. Department of Radiology, University Hospitals Leuven, Leuven, Belgium.

Head and neck cancer imaging M. Lemort¹

As it concerns tumor identification, assessment of local extent and T staging, both Computed Tomography (CT) and Magnetic Resonance (MR) are extremely well performing to give the surgeon the best view be-

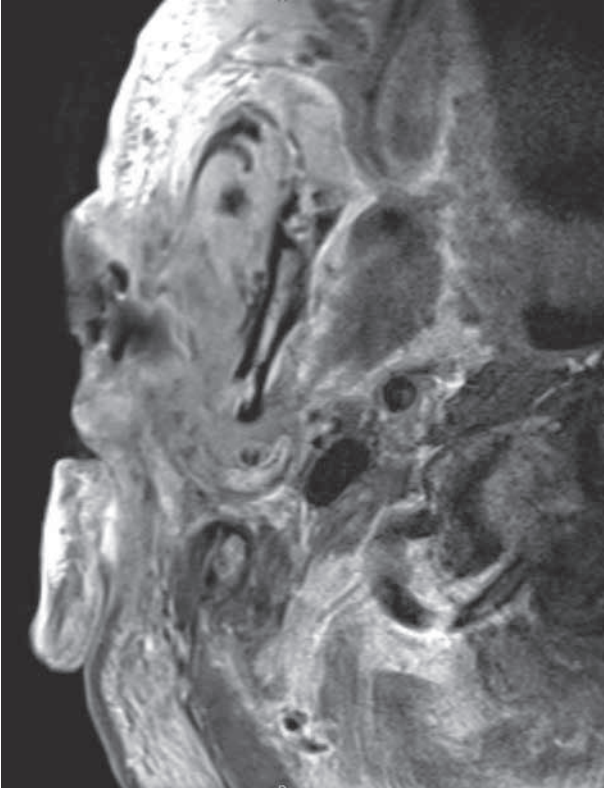


Fig. 1. — Recurrence of a basal cell carcinoma. T1-weighted post Gd FSE sequence obtained at 3.0 T with parallel imaging and surface coil. Note the minute disruption of the mandible cortical bone.

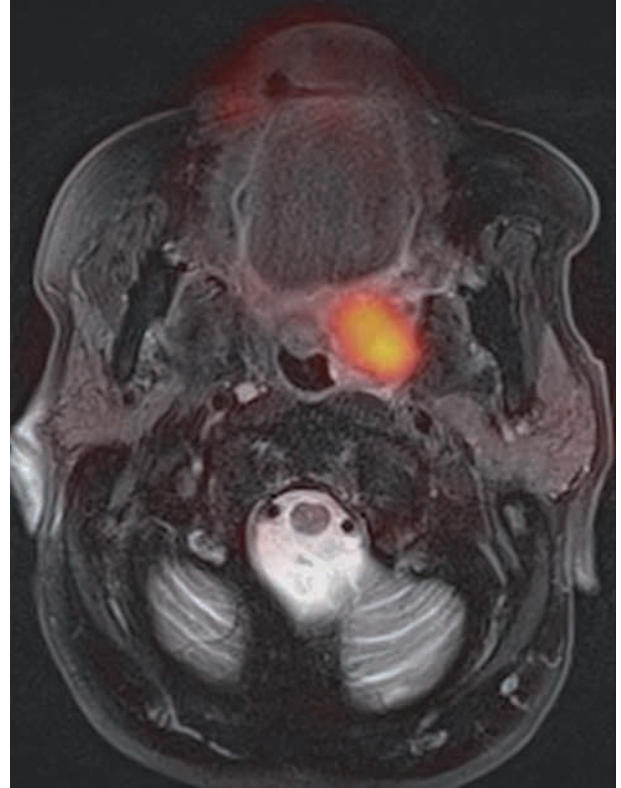


Fig. 2. — Non Hodgkin lymphoma of the left tonsil. Fused image from FDG PET and T2W FSE MRI with fat saturation.

fore surgery, if this is the treatment of choice. They may be performed either alone or in combination, the choice being dependent from the anatomical site of the lesion and the clinical condition of the patient. The quality of morphological depiction of the tumor is permanently improving with technical refinements: ultra-fast imaging at high resolution for CT, new sequences and faster techniques for MRI, together with improvement in resolution and 3D acquisition (Fig. 1).

However, morphological information on local extent is not the only point of concern in multidisciplinary discussion. Combination of therapies and the appropriate sequence of chemotherapy, radiotherapy, and/or surgery is largely depending of regional evaluation, particularly for nodal metastases, which are a remaining weakness of CT and MR, despite the initial hope placed in diffusion weighted imaging (DWI) techniques, which are still under evaluation. FDG PET-CT has only partly fulfilled this expectation. Furthermore, as oncology enters in an era of individualized treatment options depending of factors related to the biology and microenvironment

of the tumors, new imaging markers are needed to predict response.

Another challenging point is the monitoring of patient after treatment and particularly the early detection of recurrence, which may be an utmost important point not only to improve survival, but also to achieve the best quality of life for the patient along the course of the disease.

MR DWI and dynamic contrast-enhanced (DCE) MRI are under investigation for at least three main indications:

- Detection of metastatic lymph nodes (even in sub-centimetric nodes)
- Detection of recurrence in post-therapeutic follow-up (differential diagnosis between fibrosis, necrosis, and recurrence)
- Prediction and/or follow-up of response to treatment

For invaded lymph node detection, DWI probably is most valuable for squamous cell carcinoma (SCC) and moderately small nodes (4 to 10 mm) in combination with morphological imaging at N staging (1). Sufficient evidence is lacking however, and more prospective studies are needed.

DWI or DCE MRI may also be useful in case of suspected post-treatment recurrence, or standard post-treatment planned examinations and may complement a positive post-treatment PET to improve specificity (2). In addition, it may be an alternative to PET for late recurrences since PET-CT is less efficient for this indication.

There is a rationale and preliminary evidence to include new imaging biomarkers as DWI or DCE-MRI in treatment evaluation and/or planning for head and neck patients. A lot of work has to be done to ensure minimal standardization and quality control for these methods before they can be included in clinical research as surrogate markers.

DCE CT thanks to the extremely high speed of the last generation of CT devices could also be used for assessment of tumor perfusion for predicting sensitivity to radiotherapy or response to anti-angiogenic drugs. It could be easier to set up and perform in these patients than DCE MRI.

Recent introduction of fast dual-energy CT devices could also open new opportunities in tumor assessment and reduction of the needed dose of contrast media (3).

Finally, hybrid technologies such as combined PET-MRI should also bring new opportunities in head and neck cancer imaging (Fig. 2).

Head and neck cancer imaging remains an ever-changing and challenging field that promises exciting evolution in the following years.

References

1. Vandecaveye V, De Keyzer F, Vander Poorten V, Dirix P, Verbeken E, Nuyts S, et al. Head and neck squamous cell carcinoma: value of diffusion-weighted MR imaging for nodal staging. *Radiology*. 2009;251:134-146.
2. Furukawa M, Parvathaneni U, Maravilla K, Richards TL, Anzai Y. Dynamic contrast-enhanced MR perfusion imaging of head and neck tumors at 3 Tesla. *Head Neck*. 2013, 35:923-929.
3. De Cecco CN, Darnell A, Rengo M, Muscogiuri G, Bellini D, Ayuso C, et al. Dual-Energy CT: Oncologic Applications. *AJR*, 2012, 24;199(5_Supplement):S98-S105.

1. Dpt of Medical Imaging, Institut Jules Bordet, Brussels, Belgium.

Noninvasive imaging of the neck vessels: focus on treatment-oriented imaging of the carotid artery P. Vanhoenacker, P. Leyman¹

Non-invasive imaging of the internal carotid arteries (ICA) is indicated in several clinical settings:

1. Patients undergoing evaluation for acute stroke.
2. Transient ischemic attacks (TIA)
3. Cervical bruits
4. Prior to coronary artery bypass graft surgery: controversial

The choice of modality for non-invasive carotid artery assessment depends on the clinical indications for imaging and the skills available in individual centers. In our hospital, ultrasound (US) of the carotids forms the mainstay of carotid imaging, whereas CT angiography (CTA) and MR Angiography (MRA) are problem-solving modalities.

Ultrasound

Carotid duplex ultrasonography (US) is the standard of care for the initial diagnosis of carotid artery bifurcation disease.

Meta-analyses of published criteria for CDUS have demonstrated sensitivities of 98% and specificities of 88% for detecting > 50% ICA stenosis; and 94% and 90% respectively for detecting > 70% ICA stenosis

Utilizing gray-scale B-mode imaging, color and Doppler flow provide all of the imaging tools required to determine the severity of ICA stenosis. The absence or presence of hemodynamically significant disease in the ICA is determined by an increase in Doppler-derived blood flow velocity. Therefore, the accuracy of the exam is dependent upon the accuracy of the spectral Doppler waveform interrogation, which is the single most important criterion for treatment decisions.

Plaque imaging is promising but so far has little clinical value and plays no important role in treatment decisions.

Technique, pitfalls and interpretation will be demonstrated.

MRA

The techniques used for carotid MRA are time-of-flight imaging (TOF-MRA), either with 2D or 3D acquisition, and gadolinium contrast enhanced angiography (CEMRA). TOF-MRA relies on the movement of magnetized blood through the volume being imaged. CE-MRA is less dependent on blood flow for vascular contrast, and gives better visualization of the arterial lumen. CE-MRA tends to overestimate the degree of stenosis (compared with DSA), but the rate of misclassification appears to be low enough to neutralize the risks of conventional catheter angiography.

Some pitfalls, post-processing techniques and an integration algorithm with US will be presented.

Blood pool agents are promising and allow imaging with higher resolution.

Plaque imaging is promising, but as in US remains largely a research tool.

CTA

CTA has several advantages over DUS and MRA for carotid imaging:

- It has better overall spatial resolution than MRA
- It is less susceptible to artifacts than MRA
- it provides information about surrounding anatomy, such as osseous structures, useful in surgical planning
- Because CT has high spatial resolution and is unaffected by slow flow, CTA is the most appropriate non-invasive method to differentiate between near-occlusion and occlusion

Disadvantages include

- Heavy, circumferential calcification of the ICA can cause beam hardening artifact. This can be alleviated to some extent by the use of double-energy CT.
- risks associated with the use of iodinated contrast agents and radiation exposure to radiosensitive tissues (lenses and thyroid gland)

Plaque imaging with CT is not well established. The role of vasa vasorum has been studied and enhancement of the vasa vasorum adjacent to severe carotid plaque during arterial phase CTA suggests a higher likelihood of symptomatic disease (TIA or stroke).

Conclusion

Safe, accurate and reliable carotid imaging is critical in treatment of stroke caused by carotid disease. Initial imaging is done with high-quality US. MRA or CTA may be helpful in providing ancillary information to assist in planning therapy. All non-invasive imaging modalities have limitations, and imagers must appreciate them, in order to provide optimum care.

1. Dpt of radiology, OLV Ziekenhuis Aalst, Aalst, Belgium.

New trends in radiation protection for diagnostic medical exposures L. Van Bladel¹

A first part of the talk will be devoted to recent findings and interpretations that arise from the sciences underpinning radiation protection. Both advances in radiobiology and epidemiology will be discussed.

A second part will be devoted to observations with regard to medical imaging practice in Europe and beyond from the perspective of radiation protection. We will take a closer look at examination frequencies and at typical doses that result from given types of examinations.

There will be a short reminder on the system of radiation protection and how it is developed at international level. This part will be completed by challenges for radiation protection that result from recent developments in imaging practice. The conclusions and "call for action" of IAEA's International Conference on Radiation Protection in Medicine, held in December 2012 in Bonn, Germany, will be presented.

The recently approved draft European Directive that modifies the current Directive 97/43/Euratom (medical exposures or "med" directive) will be discussed, in particular where new requirements could have direct implications for daily radiological practice.

Finally, we will discuss the policy of the Belgian radiation protection competent authority, its involvement in HERCA, the European umbrella organisation, the recent achievements and on-going discussions at national, European and international level.

1. Federal Agency for Nuclear Control, Brussels, Belgium.

Dose reduction strategies in CT imaging

F. Zanca¹

In the past years, concerns have been raised regarding the potential risk of cancer induction from computed tomography (CT), due to its exponentially increased use in medicine. While there is no doubt regarding its clinical benefit when used for appropriate indications, keeping radiation dose as low as reasonably achievable remains fundamental for decreasing such risk and increase patient protection.

There are several way to reduce patient dose in CT. The first is independent of the CT scanner technical parameters and relates to the concept of justification. Indeed, the main principles proposed by the International Commission on Radiological Protection (ICRP) as applicable to patient protection are justification and optimization. Justification requires that the net benefit to be positive and its implementation in clinical practice is mainly based on the application of referral guidelines for medical imaging. This has been addressed by several organization, as the European Commission or national organizations, e.g. the Belgische Consilium Radiologicum (1).

Unfortunately, a correct use of referral guidelines remains a challenge for the healthcare systems, due to its impact on the workflow, resources and costs. For example, brain CT still makes a large part of our daily clinical practice, while it has been shown that -according to the guidelines- many CT brain examinations could be replaced by MRI. The higher cost, the lower availability of MRI and the need to help the patient immediately makes this choice less probable.

Important to remember is that justification is in the hands of the professionals rather than of the competent regulatory authority: it is a shared responsibility between referring physician and radiologist.

Once referral for CT examination has been justified, the radiologist has to ensure that the examination is carried out with a good technique, this has to do with the optimization process. Within this process the radiation dose to the patient should be limited, while providing sufficient image quality. Possibilities for dose reduction relates to standard rules like minimal anatomical length of the imaging, patient positioning at isocenter, reducing the reference tube load setting or reducing the number of multiphase images, which should always be applied. Indeed patients undergoing CT examinations may be exposed to high doses even with an optimized protocol, just because such simple methods are overlooked. For example, with the introduction of faster and faster devices with higher tube load performance, there is a tendency to extend the imaging area beyond the area of interest, with the consequence of an unnecessary extra dose (2).

Next, even when these conditions are met, there are additional opportunities to reduce dose which mainly relates to technical innovations as proposed by manufacturers: automatic tube current modulation (TCM), (automatic) selection of tube potential, adaptive collimation, new reconstruction algorithms (e.g. iterative reconstruction techniques) and protocol tailoring to patient size and age (3).

All these aspects of dose reduction strategies in CT will be discussed and some results of ongoing studies will be reported, as summarized below.

STUDY 1 Inner ear CT imaging: influence of iterative reconstruction techniques on dose and image quality

In this study we assessed the potential of Sinogram Affirmed Iterative Reconstruction (SAFIRE) relative to filtered backprojection (FBP) in terms of dose and image quality (IQ), for temporal bone computed tomography (CT).

Two cadaver heads were scanned on 128-slice multi-detector-row CT (SOMATOM Definition Flash) using the standard-of-care inner ear protocol (140 kV, 220 fixed mAs) and dose reduced protocols at 200, 180 and 160 mAs (10, 20, 30% dose reduction

respectively). In addition, the standard-of-care with lower potential (120 kV) but higher mAs (250) (30% dose reduction) was also used. Data were reconstructed with FBP and SAFIRE (strength 5), using very sharp filters. Objective and subjective measurements were performed to assess image quality. Specifically, objective noise and Hounsfield units were measured in the native axial (0.4 mm slice, 0.2 mm increment) and reformatted coronal and axial (0.8 mm slice, 1 mm increment) temporal bone images. Signal and noise were calculated and the two techniques were compared (Student t-test). For the subjective evaluation of image quality, two experienced head and neck radiologists assessed the images for visibility of ear structures and for diagnostic acceptability, using a 5-point scale (1 = insufficient; 5 = excellent).

Results shows that objective noise was significantly lower for SAFIRE respect to FBP for the native images (117 ± 6.6 vs 132 ± 8.1 , $p < 0.01$), while for the reformatted images no difference was observed between FBP and SAFIRE ($p > 0.05$). The signal followed the same trend. Subjective image quality instead was significantly better for FBP (p -value < 0.001 , SAFIRE median score 3 vs 4 for FBP). The highest average IQ score (4.5) was observed for the routine and for the 120kV protocol. Being the latter associated with a 30% dose reduction respect to the routine protocol, it became the clinically in use protocol.

In conclusion, compared to FBP, SAFIRE enabled significant reduction of objective image noise for the high resolution native images. However, overall image quality was significantly better for FBP, possibly because of the extreme strength of 5 for SAFIRE and of the images reformatting. In future lower strength of SAFIRE should be assessed and axial native images could be used instead of the reformatted ones.

Figure 1 (left) shows the measured noise in the images as a function of dose (each dose level represent a protocol) for both FBP and SAFIRE images; on the right the average score for the subjective IQ evaluation is shown, also as a function of dose. As it can be seen the protocol using lower kV (120) and higher mAs (250) shows a comparable image quality to the routine one, but having a lower CTDIvol (55 mGy instead of 75 mGy).

STUDY 2 Dose to radiosensitive organs during routine chest CT:

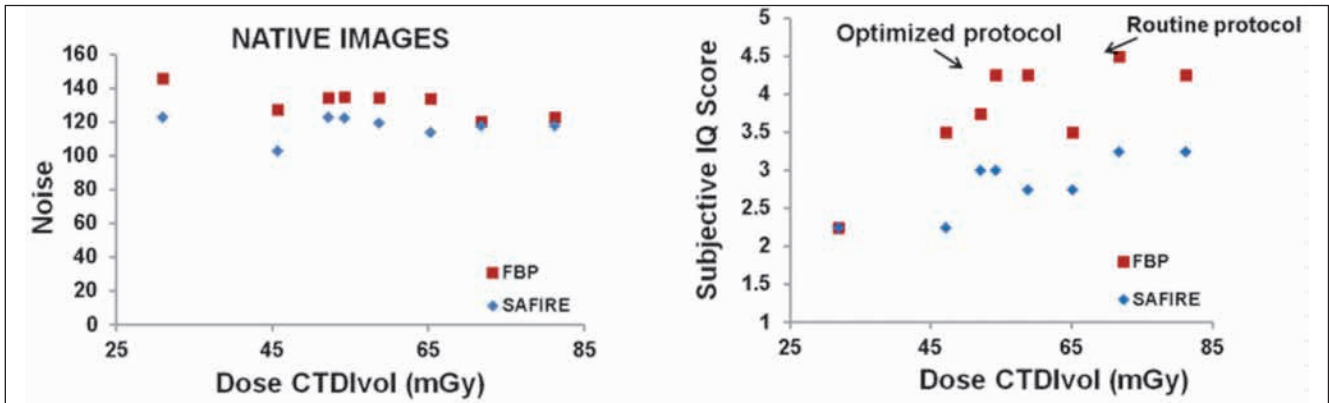


Fig. 1. — Measured noise in the images as a function of dose for FBP and SAFIRE images.

effects of standard and organ-based tube current modulation

The aim of current study was to quantify the effect of standard and organ-based tube current modulation (TCM) on dose to radiosensitive organs (breasts, lungs, heart, thyroid gland) and on image quality in adult female patients of various sizes undergoing chest CT examinations.

Four (underweight, normal, overweight and obese BMI index) female cadavers (< 24h) were scanned on 128-slice multi-detector-row CT (SOMATOM Definition Flash) using the standard-of-care protocol (with 4D CareDose TCM) and the X-Care protocol (an organ based TCM approach to reduce direct X-ray exposure for the breasts and thyroid gland). For the comparison in this work, the scanner output (CTDIvol) was matched between the two protocols. Patient and organ doses (breasts, lungs, heart and thyroid) were estimated using PCXMC 2.0 (STUK, Helsinki, Finland), which allows to rescale the phantom according to the patient's height and weight and to account for TCM. Doses were then plotted as a function of patient's BMI and regression analysis was applied. Image quality was evaluated by measuring the noise (standard deviation of CT numbers) within the lung and heart regions.

Results shows that while total mAs delivered per 360° is unchanged with organ-based TCM, patient effective dose was reduced respect to the standard protocol and the reduction decreased in function of patient size ($R^2 = 95\%$, range 25% to 4% dose reduction). The dose to the breasts, lungs, heart and thyroid was also decreased, due to the lower amount of x-rays to the anterior respect to the posterior side of the patients and

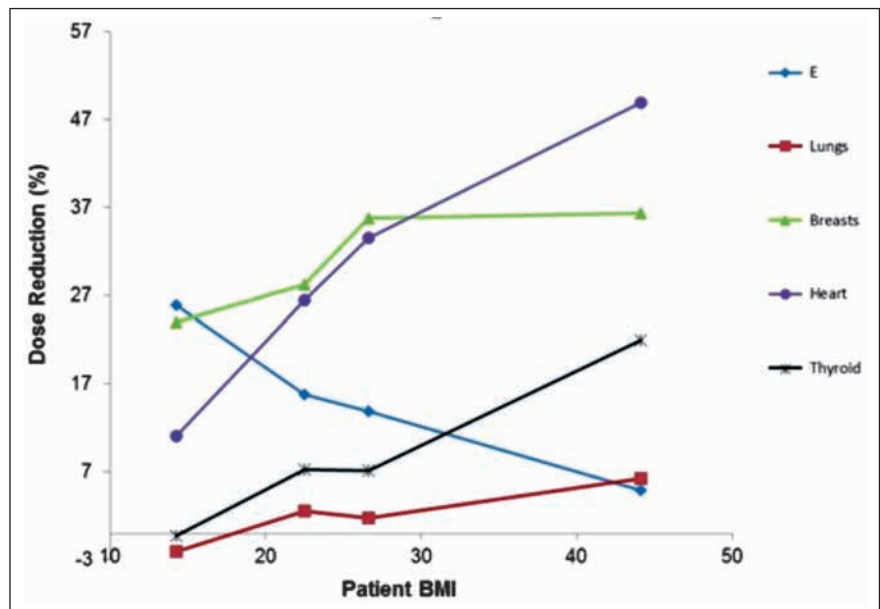


Fig. 2. — Graph showing the dose reduction (%) with organ-based TCM respect to the standard protocol for patient dose (E) and organ dose (lungs, breasts, heart, thyroid).

showed an increasing trend with patient size, ($R^2 = 92\%$, range 23%-36% for breasts, $R^2 = 84\%$, range -2% to 6% for lungs, $R^2 = 92\%$, range 11% to 48% for the heart and $R^2 = 85\%$, range 0% to 21% for the thyroid). Noise was not significantly increased ($p > 0.05$) with organ-based TCM.

In conclusion, compared with routine TCM, organ-based TCM allows for reduction of organ doses (breasts, lungs, heart and thyroid) in chest CT and the reduction increases with patient size. Indeed the higher tube current in the posterior views is contributing to the organ doses more in small (less attenuating) patients. Patient dose is also reduced but the effect is smaller for larger patients.

Image quality was not affected.

References

1. <http://www.riziv.be/care/nl/doctors/promotion-quality/guidelines-rx/pdf/guidelinesnl.pdf> (accessed on 25/09/13)
2. Zanca F, Demeter M, Oyen R, Bosmans H. Excess radiation and organ dose in chest and abdominal CT due to CT acquisition beyond expected anatomical boundaries. *Eur Radiol*, 2012 Apr, 22(4):779-88.
3. Radiation Dose from Multidetector CT, Editors: D. Tack, M. K. Kalra, P. A. Gevenois. Springer, 2012.

1. Radiology Department UZ Leuven & Imaging and Pathology Department, KUL, Leuven, Belgium.